Performance of neutron guide systems for Low Energy Accelerator-driven Neutron Facilities

Z. Ma[a,b], K. Lieutenant [b], J. Voigt [b], T. Gutberlet [b], M. Feygenson [b], T. Brückel [b]

[a] Engineering Research Center for Neutron Application, Ministry of Education, Lanzhou University, Tianshui South Road No. 222, 730000 Lanzhou, China

[b]Jülich Centre for Neutron Science, Forschungszentrum Jülich, 52425 Jülich, Germany

ABSTRACT

Low Energy accelerator-driven Neutron Facilities have the potential to become competitive to research reactors and spallation sources to generate neutron beams for scattering experiments. A low energy accelerator-driven neutron facility is developed at the Jülich Centre for Neutron Science. This source is expected to provide thermal and cold neutrons with high brilliance and is therefore called “High Brilliance neutron Source” (HBS). In this work, we study the performance of neutron guide systems at HBS by using neutron ray-tracing simulations. Elliptical and ballistic guides with elliptic diverging/converging section have been used in simulations for various moderator-to-guide distances and guide entrance cross-sections. Results show that the beam properties have a strong dependence on the distance between guide entry and moderator. We demonstrate that the ballistic guide system can achieve a comparable neutron flux and brilliance transfer as the true elliptical guide for thermal neutrons if a proper distance between guide entrance and moderator is chosen. For low-divergence cold neutrons, the selected ballistic guide is showing even better performance than the elliptical one.

Highlights:

- Elliptic and ballistic guides can both achieve a high brilliance transfer of guides installed at low energy accelerator-driven neutron facilities.
- Both guides are suitable for sources with a radius down to 1 cm.
- The beam properties have a strong dependence on the distance between guide entry and moderator.

Keywords:

Neutron guide, neutron ray-tracing simulation, VITESS, low energy accelerator-driven neutron facility

1. INTRODUCTION

With the recent loss of reactor-based neutron sources in Europe, the development of low energy accelerator-driven neutron facilities is of growing importance [1,2]. Compared with reactors and spallation neutron sources, low energy accelerator-driven neutron facilities can be built at reasonable low-cost maintenance efforts and without a nuclear licensing procedure. The Jülich Centre for Neutron Science (JCNS) investigates the concept of a powerful low energy accelerator-driven neutron facilities called “High Brilliance neutron Source” (HBS), which is aiming at a performance comparable to existing reactor and spallation neutron sources [3].

The HBS project suggests to use a proton beam of about 100 kW time-averaged power for each of its target stations. As shown in Fig. 1, the proton beam is sent simultaneously to three different targets through a multiplexer in the beam transfer system. For the Conceptional Design Report (CDR) [3], the pulse lengths were set to 52 µs, 208 µs, and 833 µs to fulfill requirements for different neutron scattering instruments. The repetition rates were adopted to the pulse lengths in order to achieve the same average power with a duty cycle of 2% yielding target stations with repetition rates of 384 Hz (t=52 µs), 96 Hz (t=208 µs), and 24 Hz (t=833 µs).

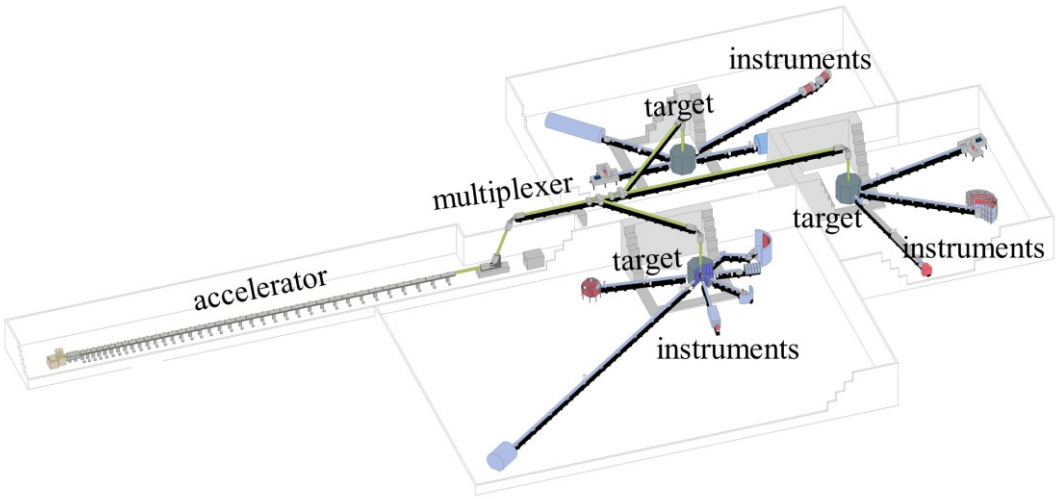

Fig. 1: Schematic layout of the accelerator-driven high brilliance neutron source HBS

The target of the HBS will be built as compact as possible to achieve high brilliance. The schematic layout of the HBS target station is shown in Fig.2. A compact, internally cooled tantalum target is designed to ensure safe and reliable operation. To achieve a high density of thermalized neutrons, which can efficiently be extracted and directed towards the instruments, a high-density hydrogen-rich thermal moderator will be used to moderate the primary neutrons into the thermal energy range in a volume as small as possible. For low and intermediate

frequencies, it is surrounded by a reflector material that sends back the neutrons escaping from the moderator region with a high probability. The internally cooled target is inserted into the thermal moderator so that the primary neutrons generated at the target are emitted preferentially towards the center of the thermal moderator.

To optimize the brilliance for cold neutrons, a cryogenic moderator will be embedded in the thermal moderator. Liquid para-hydrogen moderators offer the potential to realize a 1-dimensional source of cold neutrons, and a so-called 'Finger' moderator is proposed in HBS [4,5], following a similar strategy as for the European Spallation Source butterfly moderator (2D) and the new tube moderator for the second target station at Spallation Neutron Source (also 1D) [6–8].

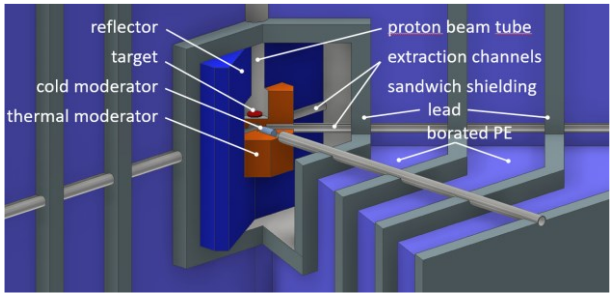

Fig. 2: Scheme of the HBS target station

The instruments are grouped around each target station operating at different frequencies to offer optimized neutron pulse structures for the individual instrument classes. Each beamline can be equipped with a dedicated thermal or cold moderator system to fulfill the requirements of the instrument installed [3]. In comparison to spallation and reactor neutron sources [9,10], HBS produces fewer fast neutrons and less amount of high energy radiation, enabling the use of a compact moderator and shielding structure [4,5]. Therefore, the guide system can be located close to the moderator and a larger phase space volume can be extracted [11–13]. In particular, this is of paramount importance for a small source size, as the phase space volume which can be loaded into a neutron guide at a certain distance is limited.

Neutron guides are used to efficiently transport neutrons from a source to a neutron scattering instrument. A very efficient guide design with ballistic geometry was introduced by Mezei [14] and installed at existing instruments [15]. This ballistic guide design consists of a linearly tapered initial section, straight middle section, and linearly tapered end section. Such design reduces the neutron losses, especially for long-wavelength neutrons in long guides. The idea is to increase the cross-section and to reduce the divergence at the beginning of the guide, which both reduces the number of reflections and thus the neutron losses. The additional gain comes from the lower reflection angle, which allows reducing the m-value of the coating and reduces the costs as well as the losses in each reflection [16]. One step further in this direction would

be to use parabolic shapes for the diverging and converging sections to make the beam parallel and finally focus it again [17].

The next idea was to use an elliptical guide to reduce the number of reflections to one per dimension, .i.e. usually two [17], as realized at the instrument HRPD at ISIS [18]. The next idea was to use a double elliptic guide because a single guide inverts the phase space and the second ellipse recovers it, so-called the SELENE principle [19]. This concept was used for the POWTEX instrument at FRM II reactor [20]. The search for the ideal connection of the two ellipses finally leads to the design of a guide of elliptic shape in the first and fourth quarter and a constant cross-section in the second and third [21].

Systematic comparisons of different shapes showed that the gain can be huge, but depends on the wavelength range and needed divergence and that the advanced shapes are indeed superior to the original ballistic guide [22]. While the elliptic shape often gives the highest flux at the sample, it has the disadvantage that the divergence distribution is often inhomogeneous [23] and the sample is in direct line of sight [24]. The latter problem also occurs if parabolic shapes are used, or more generally if the shape of the lateral cut has a kink [22]. This favors guides with half an ellipse in the first and the last sections [13]. Numerical optimization of the guide shape also gives elliptic or elliptical-ballistic guide shapes [25].

While the performance has been thoroughly studied for existing neutron sources with large moderators and long moderator to guide distances, it is not clear what is the optimal shape, size, and moderator to guide distance for low energy accelerator-driven neutron facilities, where the distance can be small, e.g. 30 cm. In this work, we explore systematically the potential of elliptical and elliptic-ballistic guides with parameters of a compact source (of radius 1 cm) with a special emphasis on the flexibility in the moderator-to-guide distance. We focus on elliptic and ballistic shapes with elliptic sections at the entrance and exit, which have proven to perform very well at reactor and spallation neutron sources for extended and 2D moderator geometries. Our results indicate that with the small source and short moderator guide distance, a ballistic guide with a long elliptical converging/diverging part has a performance comparable to that of an elliptical guide.

2. SIMULATION SETUP

Among the various instruments proposed for the HBS [3], a 60 m long medium-resolution Disordered Materials Diffractometer was designed for the study of small samples of nanoscale and disordered materials with a high neutron flux. It uses the entire pulse and requires a neutron guide long enough to reach a medium-Q resolution at 60 m. This rather simple and robust

concept can be easily adapted by other instruments and thus, it was chosen as the first HBS beamline to be simulated with the neutron ray-tracing method [26].

According to the current design, a wavelength band chopper will be set about halfway between the moderator and detector and a frame overlap chopper will be set just outside of the shielding block, i.e. 2 m from the moderator surface. The moderator-to-sample distance is 59 m. The low particle energy of HBS compared to spallation sources results in expected less background which is hopefully acceptable for instruments. The problem of the direct line of sight between the moderator and sample and its impact on the background are not investigated in this work and it would be discussed in future full instrument concept design.

In the simulations, the moderator has a diameter of 2 cm and neutrons are emitted from the moderator surface, the pulse repetition rate is 96 Hz, yielding a bandwidth of $\Delta\lambda \approx$ 0.7 Å. The sample size is 1×1 cm^2, the total neutron flux into 2π at the moderator is set to 4×10^{12} $n\cdot s^{-1}\cdot cm^{-2}$.

Fig. 3 shows three different types of geometries considered in our simulations, all with a square cross-section:

(a) An elliptical guide of m = 5 coating. (As state-of-the-art neutron guides of high m-coating have the same reflectivity as low m-coating guides for low Q, it is straightforward to perform simulations with high m-coating and reduce the coating in the last development step to the needed value.)

(b) A 3-section ballistic guide that uses an elliptical diverging section, a straight section, and an elliptical focusing section of length ratio 1:2:1 (c.f. Fig. 3). An m = 5 coating is used for the whole guide. The elliptical sections end/begin at their maximal cross-section to avoid a kink in the guide profile. For simplicity, this type of guide is named 1/4 ballistic guide.

(c) A 3-section ballistic guide that uses an elliptical diverging section, a straight section, and an elliptical focusing section of length ratio 1:4:1. Otherwise, it has the same properties as the 1/4 ballistic guide. This type of guide is named 1/6 ballistic guide.

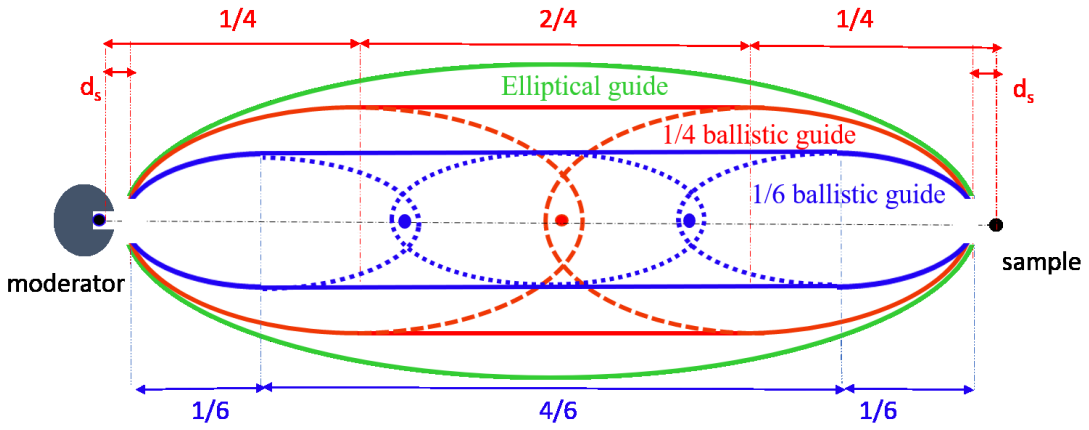

Fig. 3: Schematic of the neutron guides used in the simulations. Green: elliptical guide, red: 1/4 ballistic guide with elliptic opening and focusing sections, blue: 1/6 ballistic guide, also with elliptic opening and focusing sections. The filled circles indicate the focal points, moderator surface and sample are set at the focal point.

The entrance and exit cross-sections of the guide system are always identical and are chosen to be either 2 × 2 cm^2 or 3 × 3 cm^2. Moderator surface and sample are placed at the focal points of the corresponding ellipses. With the focal points fixed (at source and sample) and the concept to use 2 half-ellipses, there are only 2 degrees of freedom: the width of the guide and the length of the ellipse. For both parameters, we used different values.

The distance from the source to guide entry position d_s is the same as the distance from guide exit to sample position. This distance d_s is changed from 30 cm to 140 cm in 10 cm steps. 72 configurations were investigated in total. The maximum heights of these guides are shown in Fig. 4. The spatial distribution is monitored at the sample position; and the flux, the divergence distribution, and the brilliance within the sample area are also monitored. The Monte-Carlo simulations are performed by using the simulation program VITESS [26].

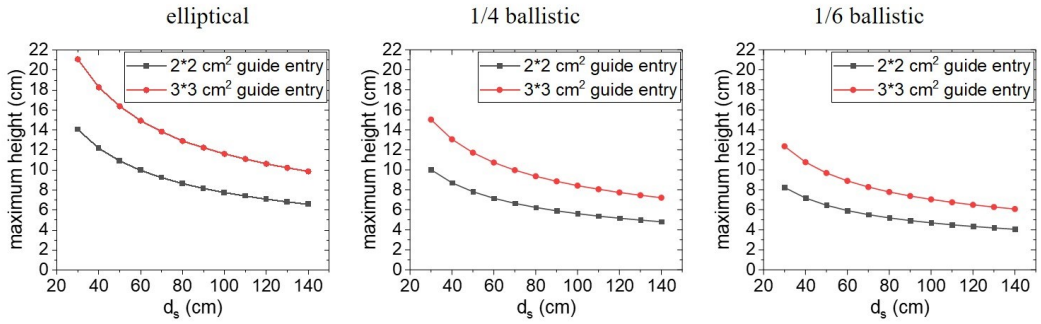

Fig. 4: The maximum height of the guide as a function of the distance d_s.

3. RESULTS AND DISCUSSION

3.1 Flux

Fig. 5 shows the neutron flux at the sample position for different guide shapes and a wavelength range of 0.5 Å < λ < 1.2 Å. For the true elliptical guide, the 2 × 2 cm^2 entrance yields a higher flux compared with a 3 × 3 cm^2 guide if d_s < 70 cm, while the neutron guide with 3 × 3 cm^2 cross-section gives a higher flux for larger distances. For the 1/4 ballistic guide, the guide with 2 × 2 cm^2 entry can achieve a higher flux compared with a 3 × 3 cm^2 cm guide if d_s < 110 cm; for larger distances, the neutron flux is nearly the same for both entrance sizes. For the 1/6 ballistic guide, the guide with a 2 × 2 cm^2 entrance gives a higher flux at the sample compared with a 3 × 3 cm^2 guide entrance if the distance is below 90 cm; if the distance is increased, it results in a lower flux.

For the guide shapes used in the simulations, the flux at the sample is first increasing with d_s

and then decreasing after reaching a maximum. For the true elliptical guide, the highest neutron flux of (8.55 ± 0.02) × 10^7 n·cm^{-2}·s^{-1} is obtained with 2 × 2 cm^2 guide entry and for 40 cm distance. For the 3×3 cm^2 guide entrance, the neutron flux at the sample is highest with (7.14 ± 0.02) × 10^7 n·cm^{-2}·s^{-1}for a distance of 60 cm. If d_s = 40 cm, the neutron flux at the sample position for the 1/4 ballistic guide with 2 × 2 cm^2 guide entry is about (7.99 ± 0.02) × 10^7 n·cm^{-2}·s^{-1}, which is 93.4% of the neutron flux of the elliptical guide at the sample position. For the 1/6 ballistic guide with 2 × 2 cm^2 and d_s = 50 cm, the neutron flux at the sample position is about (6.49 ± 0.02) × 10^7 n·cm^{-2}·s^{-1}, which is 76% of the maximal neutron flux of the elliptical guide at the same sample position.

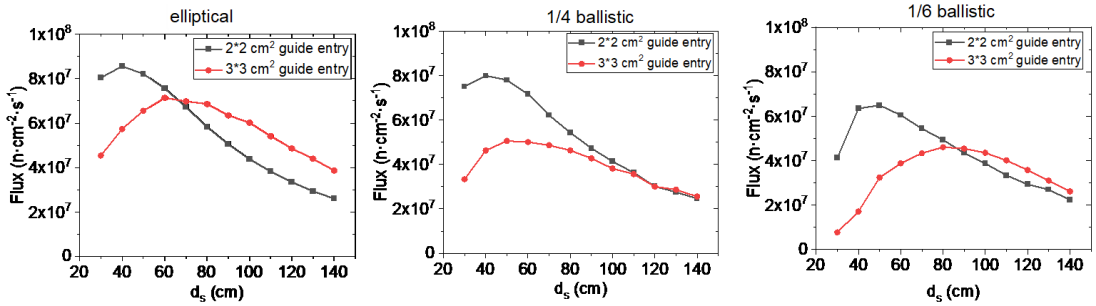

Fig. 5: Neutron flux at the sample position for different types of neutron guides. The wavelength range is 0.5 Å < λ < 1.2 Å.

3.2 Spatial and divergence distribution

The spatial and the divergence distribution at the sample position for 1/4 ballistic guide with a 2 × 2 cm^2 guide entry is shown in Fig. 6 and Fig. 7 with the distance d_s between guide entry and moderator ranging from 30 cm to 140 cm. These distributions have a strong dependence on this distance. For the maximum flux (d_s = 40 cm), the spatial distribution of the neutrons at the sample position has a circular intensity plateau and the beam spot features a circular halo with a diameter of 1.6 cm (see Fig. 6), which is slightly smaller than the moderator size. One possible explanation for this result is neutrons emitted from the center of the source are more likely to be reflected and reach the center of the sample. Another possible explanation is that the guide entrance and exit used in simulation have a size of only 2 × 2 cm^2, which reduces the illumination of the edges. The reduction of the neutron intensity for d_s > 50 cm is visible in Fig. 6. Since the wavelengths used in the simulation are short (< 1.2 Å), the influence of gravity is not visible.

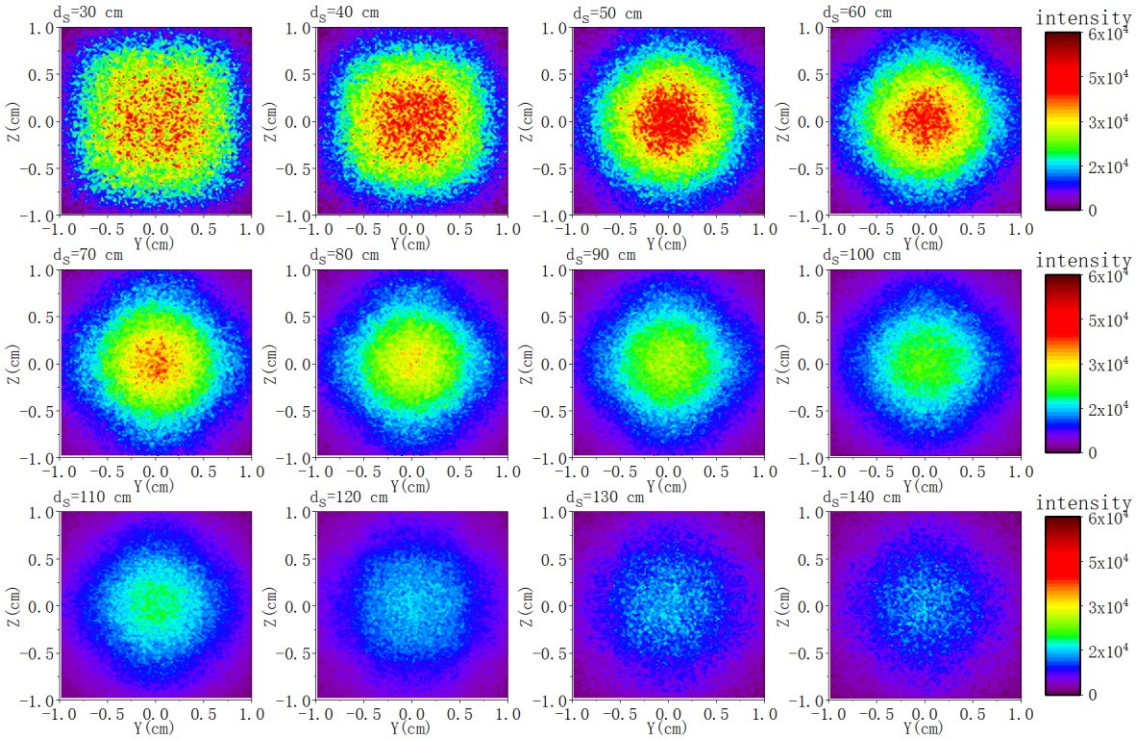

Fig. 6: Neutron spatial distribution at the sample for 1/4 ballistic guide with 2 × 2 cm^2 guide entry 30 cm ≤ d_s ≤ 140 cm from top left to bottom right. The wavelength range is 0.5 Å < λ < 1.2 Å.

As the distance between guide exit and sample position d_S is increased, the beam hitting the cross-section of 1 cm × 1 cm at the sample position becomes more and more collimated. This is reflected in the divergence distribution becoming narrower with increasing d_S, as visible in Fig. 7.

Fig. 8 shows the spatial and divergence distribution at the sample position (1 × 1 cm^2) for elliptical and 1/6 ballistic guide with 2 × 2 cm^2 guide entry and d_s = 40 cm, i.e. the setting yielding the highest flux for this guide entry size. For the full elliptic shape, the beam spot features a circular halo with a diameter of 1.6 cm, which is slightly smaller than the moderator size. The spatial distribution of the neutrons at the sample position has a diamond-like intensity plateau for the elliptical guide. For the 1/6 ballistic guide, the neutron distribution at the sample position has a squared shape. The intensity in the plateau is lower compared to the two other options and the plateau extends across a larger area of the beam spot.

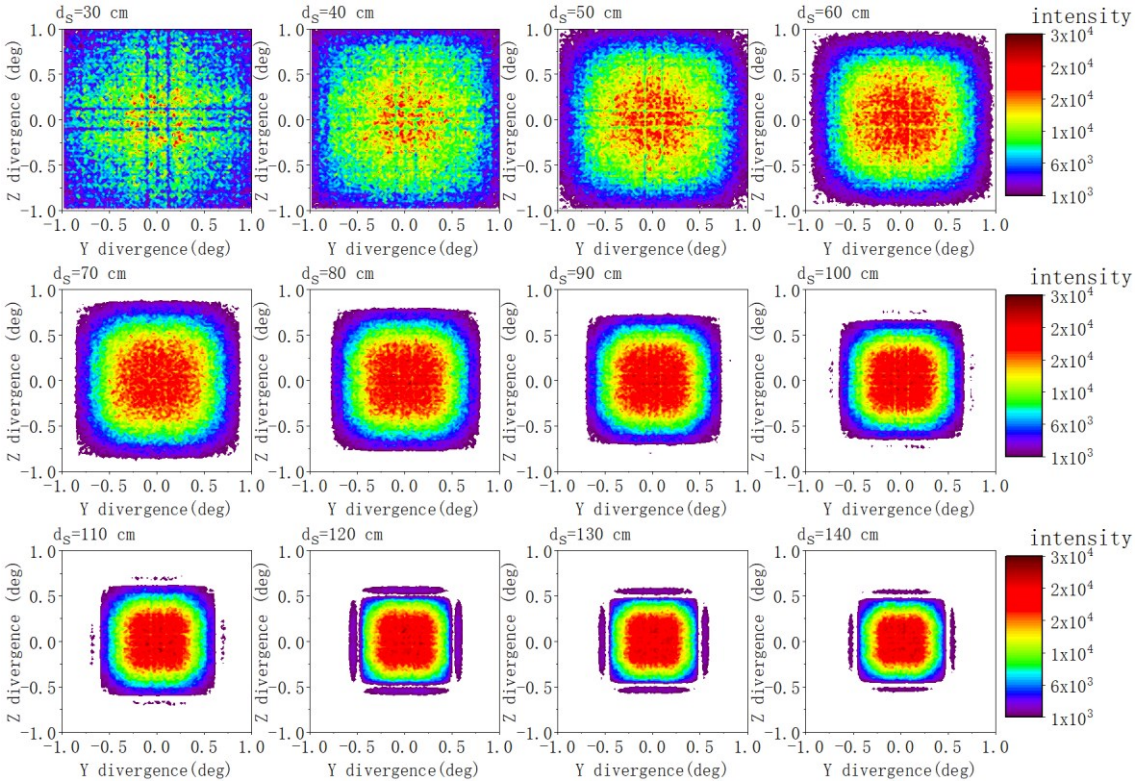

Fig. 7: Neutron divergence distribution at the sample for 1/4 ballistic guide with 2 × 2 cm^2 guide entry and 30 cm ≤ d_s ≤ 140 cm from top left to bottom right. The wavelength range is 0.5 Å < λ < 1.2 Å. The divergence distribution is shown for neutrons within a 1 × 1 cm^2 area.

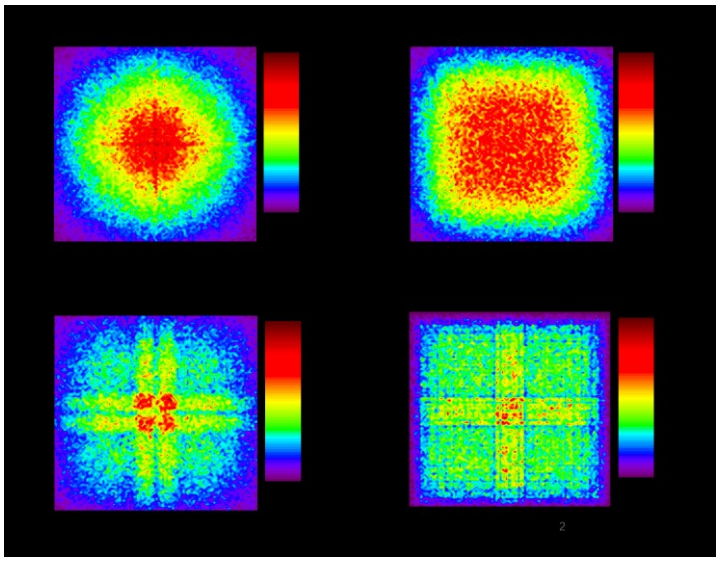

Fig. 8: Neutron spatial (a) and divergence (c) distribution at the sample for true elliptical guide; Neutron spatial (b) and divergence (d) distribution at the sample for 1/6 ballistic guide. All guides have a 2 × 2 cm^2 guide entry and d_s = 40 cm. The wavelength range is 0.5 Å < λ < 1.2 Å. The divergence distribution is shown for neutrons within a 1 × 1 cm^2 area.

The divergence distribution of the elliptical guide, shown in Fig. 8 (c), has four characteristic peaks, which are the results of the rays with one reflection per side. For the 1/6 ballistic guide, these four peaks are not found. Still, one observes a cross-shaped intensity distribution with streaks of reduced intensity for both the 1/4 and the 1/6 ballistic guides.

3.3 Number of reflections

The number of reflections of the neutron is counted by recording the times that a neutron hits the guide wall. In VITESS, the neutrons are marked by a so-called "color" and VITESS will add a value to the neutron color on each reflection. The number of reflections inside the guide is counted for the neutrons entering the sample area. Elliptical and ballistic guides with 2×2 cm^2 guide entrance and $d_s = 40$ cm are used in the simulations. A 2×2 cm^2 cross-section straight guide with $m = 5$ coating is used for comparison. The neutron counts are divided by the number of neutrons passing through the guide. Fig. 9 shows this fraction as a function of the number of reflections for the neutrons arriving in the sample area. Most of the neutrons reaching the sample area are reflected 3 or 4 times for the elliptical guide, 4 or 5 times for the 1/4 ballistic guide, 5 or 6 times for the 1/6 ballistic guide. The average reflection count for the neutron arriving in the sample area is 3.92 (σ=0.35) for elliptical guide, 4.41 (σ=0.46) for 1/4 ballistic guide, 4.91 (σ=0.50) for 1/6 ballistic guide, and 9.68 (σ=0.31) for a 2×2 cm^2 cross-section straight guide, that was simulated for comparison.

The number of reflections is significantly lower than found in guides designed for large moderators – about 7 for an elliptic shape [23]. This is not surprising because trajectories with a high number of reflections arise from starting points away from the focal point, i.e. outside the moderator center [23,28].

The theoretical numbers of reflections for neutrons starting from the focal point is 2 for an elliptic shape and 4 for a double elliptic guide, (1 and 2, respectively, per dimension). The 1/4 ballistic guide is a special case of the double elliptic guide; for the neutrons that are first reflected in the (elliptically) diverging part, which is the majority [23], the trajectories are the same. The others will also have typically 2 reflections. Therefore, the theoretical value is close to 4 here. For the 1/6 ballistic guide, the expected number of reflections is larger than 4, because the 2nd reflection is not directing the neutron towards the sample so that in many cases a 3rd reflection will be necessary resulting in an average value of about 4.5 to 5 (the exact value strongly depends on the incoming divergence and the accepted reflection angle). A comparison shows that the number obtained from simulations is in good agreement with estimated values for the ballistic guides.

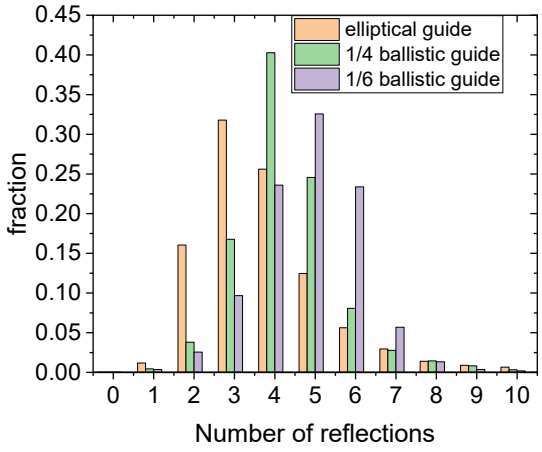

Fig. 9: The number of reflections in elliptical, 1/4 ballistic, and 1/6 ballistic guides for neutrons arriving within a 1 × 1 cm^2 sample area . All guides have a 2 × 2 cm^2 guide entry and d_s = 40 cm. The wavelength range is 0.5 Å < λ < 1.2 Å.

3.4 Brilliance transfer efficiency

The main feature of the Disordered Materials Diffractometer proposed at HBS is its ability to perform Pair-Distribution Function (PDF) measurements by utilizing short-wavelength neutrons, for which the beam transport is especially difficult. Therefore, all simulations in sections 3.1 and 3.2 were performed using its standard wavelength range of 0.5 to 1.2 Å.

Diffraction measurements with longer wavelengths can complement PDF studies of nanoscale and disordered materials. At the same time, longer wavelengths can be used for alternative instruments at HBS geared towards diffraction measurements of magnetic and large unit-cell samples. In order to gain more insights into the performance of such instruments, we performed additional simulations of the brilliance transfer in a wider range of wavelengths from 0 to 5 Å. The time structure in the beam was neglected for simplicity.

According to Liouville's theorem, the brilliance at the sample can never be higher than at the moderator surface. The brilliance transfer, which is defined as the ratio of the brilliance at the sample to that at the moderator surface, is used to provide a quantitative measure of how well the guide transports neutrons. The brilliance transfer is divergence-related, and the guide system has a different response to the low divergence neutron and high divergence neutron [22]. To determine the brilliance transfer of the guide system for different divergence range neutrons, the brilliance is recorded at a 1×1 cm^2 moderator surface and the 1×1 cm^2 sample area within a divergence range of ± 1° and ± 0.55° in both dimensions, respectively. Elliptical and ballistic guides with 2 × 2 cm^2 guide entrance and d_s = 40 cm are used in the simulations.

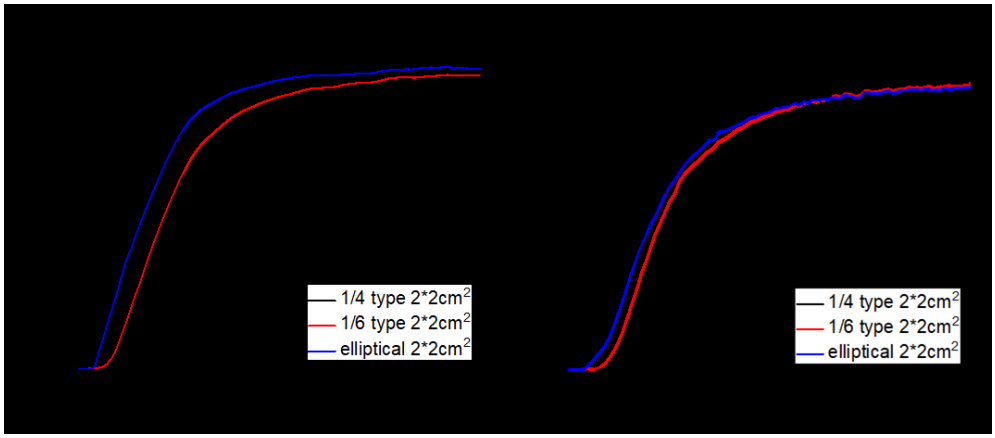

Fig. 10: Brilliance transfer as a function of wavelength of the guides with different shapes and two different divergence ranges. Left: ± 0. 55º, right: ± 1º. All guides have a 2 × 2 cm^2 guide entry and d_s = 40 cm.

The simulated brilliance transfer as a function of the neutron wavelength for three types of guides with 2×2 cm^2 guide entry and d_s = 40 cm is shown in Fig. 10. The statistical error in the simulation is less than 1%. The brilliance transfer generally increases with wavelength due to the increase in supermirror reflectivity with decreasing momentum transfer or increasing wavelength. For a divergence range of ± 0.55º, the elliptical guide has the highest brilliance transfer for short neutron wavelengths $\lambda < 1.85$ Å. At $\lambda > 1.85$Å, the 1/4 ballistic guide shows the highest brilliance transfer. The brilliance transfer of the 1/4 ballistic guide is about 93% for neutrons with $\lambda > 2.5$ Å, and the maximum brilliance transfer for the 1/6 ballistic and elliptical guides is less than 90%. Our simulations show that the optimized 1/4 ballistic guide has a higher brilliance transfer efficiency than the elliptical guide for long wavelengths.

For a divergence range of ± 1º, the brilliance transfer shows the same property. At $\lambda > 1.35$ Å, the 1/4 ballistic guide shows the highest brilliance transfer. At $\lambda > 2.5$ Å, the 1/6 ballistic guide has a higher brilliance transfer than the elliptical guide. Overall, the elliptical, 1/4 ballistic, and 1/6 ballistic guides can achieve a maximum brilliance transfer of about 87%.

The brilliance transfer of the parabolic ballistic guide, which is formed by replacing the elliptical part of the 1/4 ballistic guide with a parabolic one, has also been simulated for comparison. The results show that The brilliance transfer of the 1/4 ballistic parabolic guide is about 70% for neutrons with $\lambda > 2$ Å for the divergence range of ± 0.55º, and 58% for the divergence range of ± 1º. Namely, a ballistic guide with the parabolic end pieces resulted in lower performance compared with the elliptical end pieces, which also corresponds with previous studies for large moderators [12,29].

4. SUMMARY AND CONCLUSIONS

Detailed simulations of the different guide configurations were carried out for guides at a compact accelerator-driven neutron source. The results show that neutron beam properties at the sample position have a strong dependence on guide shape and geometry, especially the distance from moderator-to-guide entry. For a wavelength range of 0.5 Å < λ < 1.2 Å, the true elliptical guide with 2 × 2 cm^2 guide entry and exit delivers the highest neutron flux. For d_s =

40 cm and 2 × 2 cm^2 guide entry, which yields the highest neutron flux at the sample position, we obtain the flux of (7.99 ± 0.02) × 10^7 $n \cdot cm^{-2} \cdot s^{-1}$ for the 1/4 ballistic guide and (6.49 ± 0.02) × 10^7 $n \cdot cm^{-2} \cdot s^{-1}$ for the 1/6 ballistic guide within the usable wavelength band, corresponding to 96.3% and 80% of the elliptical guide flux (8.55 ± 0.02) × 10^7 $n \cdot cm^{-2} \cdot s^{-1}$ respectively.

The spatial distribution at the sample position shows that a 2 cm diameter thermal source can be imaged to a spot on the sample of about the same size or smaller by both, the elliptical and the ballistic guide systems studied. As samples are usually not larger than 2 cm and higher divergences lower the resolution, larger sources do not provide any advantage. For larger sources, this is about the size of a suggested focal point in front of the guide [30].

The simulations also show that the transport of neutrons from a small source is very efficient. For cold neutrons with ± 0.55º divergence, the maximum brilliance transfer of a 1/4 ballistic guide with 2 × 2 cm^2 guide entry and 40 cm distance reaches 93% already at a neutron wavelength > 2 Å. Note, that this is higher than that of the elliptical guide with the same guide entry and exit and the same distance. This can be related to the higher number of reflections in the ballistic guide in comparison to the elliptical one.

In summary, a 1/4 ballistic guide with an elliptical converging/diverging part can achieve comparable performance with the elliptical guide. Its advantage is the smaller guide cross-section and the simpler straight section, which together lead to a cost reduction compared to the true elliptic guide. Therefore, this guide shape can be a potential candidate for a diffraction instrument at HBS.

The beam parameters of the ballistic guides such as divergence and spatial intensity distribution are comparable to the guide systems that have been developed for more extended sources and larger distances between the neutron source and the guide system [21, 22, 26, 28]. The flux optimized designs we find here rely on short distances between the moderator and the guide system. Therefore, they are particularly suited for low energy accelerator-driven neutron facilities with their lighter shielding as compared to research reactors and spallation sources. The possibility of applying a ballistic guide with an elliptical converging/diverging part into the large moderator warrants further investigation.

ACKNOWLEDGEMENT

We thank the ‘2019 Helmholtz – OCPC – Program for the involvement of postdocs in bilateral collaboration projects’ for their financial support that enabled this important study.

REFERENCES

[1] S. Böhm, T. Cronert, J.-P. Dabrück, X. Fabrèges, T. Gutberlet, F. Mezei, A. Letourneau, A. Menelle, F. Ott, U. Rücker, Neutron Scattering Instrumentation at Compact Neutron Sources, ArXiv Prepr. ArXiv1809.02370. (2018).

[2] H. Schober, Bridging Europe’s neutron gap, Cern Cour. (2020). https://cerncourier.com/a/bridging-europes-neutron-gap/.

[3] T. Brückel, T. Gutberlet, J. Baggemann, S. Böhm, P. Doege, J. Fenske, M. Feygenson, A. Glavic, O. Holderer, S. Jaksch, M. Jentschel, S. Kleefisch, H. Kleines, J. Li, K. Lieutenant, P. Mastinu, E. Mauerhofer, O. Meusel, S. Pasini, H. Podlech, M. Rimmler, U. Rücker, T. Schrader, W. Schweika, M. Strobl, E. Vezhlev, J. Voigt, P. Zakalek, O. Zimmer, Conceptual Design Report Jülich High Brilliance Neutron Source (HBS), Forschungszentrum Jülich GmbH, 2020. https://www.fz-juelich.de/SharedDocs/Downloads/JCNS/JCNS-2/EN/Conceptual-Design-Report-HBS.pdf?__blob=publicationFile.

[4] T. Cronert, J.P. Dabruck, P.E. Doege, Y. Bessler, M. Klaus, M. Hofmann, P. Zakalek, U. Rücker, C. Lange, M. Butzek, W. Hansen, R. Nabbi, T. Brückel, High brilliant thermal and cold moderator for the HBS neutron source project Jülich, J. Phys. Conf. Ser. 746 (2016). https://doi.org/10.1088/1742-6596/746/1/012036.

[5] S. Eisenhut, M. Klaus, J. Baggemann, U. Rücker, Y. Beßler, A. Schwab, C. Haberstroh, T. Cronert, T. Gutberlet, T. Brückel, C. Lange, Cryostat for the provision of liquid hydrogen with a variable ortho-para ratio for a low-dimensional cold neutron moderator, EPJ Web Conf. 231 (2020) 04001. https://doi.org/10.1051/epjconf/202023104001.

[6] F. Mezei, L. Zanini, A. Takibayev, K. Batkov, E. Klinkby, Low dimensional neutron moderators for enhanced source brightness, 17 (2014) 101–105. https://doi.org/10.3233/JNR-140013.

[7] L. Zanini, E. Klinkby, F. Mezei, A. Takibayev, Low-dimensional moderators at ESS and compact neutron sources, EPJ Web Conf. 231 (2020) 04006. https://doi.org/10.1051/epjconf/202023104006.

[8] F.X. Gallmeier, E.B. Iverson, W. Lu, P.D. Ferguson, R.K. Crawford, SNS second target station moderator performance update, 19th Meet. Collab. Adv. Neutron Sources. (2010).

[9] K. Batkov, A. Takibayev, L. Zanini, F. Mezei, Unperturbed moderator brightness in pulsed neutron sources, Nucl. Inst. Methods Phys. Res. A. 729 (2013) 500–505. https://doi.org/10.1016/j.nima.2013.07.031.

[10] R. Gilles, A. Ostermann, C. Schanzer, B. Krimmer, W. Petry, The concept of the new small-angle scattering instrument SANS-1 at the FRM-II, 386 (2006) 1174–1176. https://doi.org/10.1016/j.physb.2006.05.403.

[11] C. Pelley, F. Kargl, V.G. Sakai, M.T.F. Telling, F. Fernandez-Alonso, F. Demmel, Guide design study for the high-resolution backscattering spectrometer FIRES, J. Phys. Conf. Ser. 251 (2010) 2–7. https://doi.org/10.1088/1742-6596/251/1/012063.

[12] R. Kajimoto, K. Nakajima, M. Nakamura, K. Soyama, T. Yokoo, K. Oikawa, M. Arai, Study of the neutron guide design of the 4SEASONS spectrometer at J-PARC, Nucl. Instruments Methods Phys. Res. Sect. A Accel. Spectrometers, Detect. Assoc. Equip. 600 (2009) 185–188. https://doi.org/10.1016/j.nima.2008.11.028.

[13] K.H. Andersen, D.N. Argyriou, A.J. Jackson, J. Houston, P.F. Henry, P.P. Deen, R. Toft-Petersen, P. Beran, M. Strobl, T. Arnold, H. Wacklin-Knecht, N. Tsapatsaris, E. Oksanen, R. Woracek, W. Schweika, D. Mannix, A. Hiess, S. Kennedy, O. Kirstein, S. Petersson Årsköld, J. Taylor, M.E. Hagen, G. Laszlo, K. Kanaki, F. Piscitelli, A. Khaplanov, I. Stefanescu, T. Kittelmann, D. Pfeiffer, R. Hall-Wilton, C.I. Lopez, G. Aprigliano, L. Whitelegg, F.Y. Moreira, M. Olsson, H.N. Bordallo, D. Martín-Rodríguez, H. Schneider, M. Sharp, M. Hartl, G. Nagy, S. Ansell, S. Pullen, A. Vickery, A. Fedrigo, F. Mezei, M. Arai, R.K. Heenan, W. Halcrow, D. Turner, D. Raspino, A. Orszulik, J. Cooper, N. Webb, P. Galsworthy, J. Nightingale, S. Langridge, J. Elmer, H. Frielinghaus, R. Hanslik, A. Gussen, S. Jaksch, R. Engels, T. Kozielewski, S. Butterweck, M. Feygenson, P. Harbott, A. Poqué, A. Schwaab, K. Lieutenant, N. Violini, J. Voigt, T. Brückel, M. Koenen, H. Kämmerling, E. Babcock, Z. Salhi, A. Wischnewski, A. Heynen, S. Désert, J. Jestin, F. Porcher, X. Fabrèges, G. Fabrèges, B. Annighöfer, S. Klimko, T. Dupont, T. Robillard, A. Goukassov, S. Longeville, C. Alba-Simionesco, P. Bourges, J. Guyon Le Bouffy, P. Lavie, S. Rodrigues, E. Calzada, M. Lerche, B. Schillinger, P. Schmakat, M. Schulz, M. Seifert, W. Lohstroh, W. Petry, J. Neuhaus, L. Loaiza, A. Tartaglione, A. Glavic, S. Schütz, J. Stahn, E. Lehmann, M. Morgano, J. Schefer, U. Filges, C. Klauser, C. Niedermayer, J. Fenske, G. Nowak, M. Rouijaa, D.J. Siemers, R. Kiehn, M. Müller, H. Carlsen, L. Udby, K. Lefmann, J.O. Birk, S. Holm-Dahlin, M. Bertelsen, U.B. Hansen, M.A. Olsen, M. Christensen, K. Iversen, N.B. Christensen, H.M. Rønnow, P.G. Freeman, B.C. Hauback, R. Kolevatov, I. Llamas-Jansa, A. Orecchini, F. Sacchetti, C. Petrillo, A. Paciaroni, P. Tozzi, M. Zanatta, P. Luna, I. Herranz, O.G. del Moral, M. Huerta, M. Magán, M. Mosconi, E. Abad, J. Aguilar, S. Stepanyan, G. Bakedano, R. Vivanco, I. Bustinduy, F. Sordo, J.L. Martínez, R.E. Lechner, F.J. Villacorta, J. Šaroun, P. Lukáš, M. Markó, M. Zanetti, S. Bellissima, L. del Rosso, F. Masi, C. Bovo, M. Chowdhury, A. De Bonis, L. Di Fresco, C. Scatigno, S.F. Parker, F. Fernandez-Alonso, D. Colognesi, R. Senesi, C. Andreani, G. Gorini, G. Scionti, A. Schreyer, The instrument suite of the European Spallation Source, Nucl. Instruments Methods Phys. Res. Sect. A Accel. Spectrometers, Detect. Assoc. Equip. 957 (2020) 163402. https://doi.org/10.1016/j.nima.2020.163402.

[14] F. Mezei, The raison d'être of long pulse spallation sources, J. Neutron Res. 6 (1997) 3–32. https://doi.org/10.1080/10238169708200095.

[15] H. Häse, A. Knöpfler, K. Fiederer, U. Schmidt, D. Dubbers, W. Kaiser, A long ballistic supermirror guide for cold neutrons at ILL, Nucl. Instruments Methods Phys. Res. Sect. A Accel. Spectrometers, Detect. Assoc. Equip. 485 (2002) 453–457. https://doi.org/10.1016/S0168-9002(01)02105-2.

[16] S. Holm-Dahlin, M.A. Olsen, M. Bertelsen, J.O. Birk, K. Lefmann, Optimization of Performance, Price, and Background of Long Neutron Guides for European Spallation Source, Quantum Beam Sci. 3 (2019) 16. https://doi.org/10.3390/qubs3030016.

[17] C. Schanzer, P. Böni, U. Filges, T. Hils, Advanced geometries for ballistic neutron guides, Nucl. Instruments Methods Phys. Res. Sect. A Accel. Spectrometers, Detect. Assoc. Equip. 529 (2004) 63–68. https://doi.org/10.1016/j.nima.2004.04.178.

[18] R.M. Ibberson, Design and performance of the new supermirror guide on HRPD at ISIS, Nucl. Instruments Methods Phys. Res. Sect. A Accel. Spectrometers, Detect. Assoc. Equip. 600 (2009) 47–49. https://doi.org/10.1016/j.nima.2008.11.066.

[19] U. Hansen, Status report on the WP2 of the Swiss-Danish instrumentation work packages for the European Spallation Source , ESS focusing reflectometer for small samples Selene guide concept, (2013).

[20] A. Houben, W. Schweika, T. Brückel, R. Dronskowski, New neutron-guide concepts and simulation results for the POWTEX instrument, Nucl. Instruments Methods Phys. Res. Sect. A Accel. Spectrometers, Detect. Assoc. Equip. 680 (2012) 124–133. https://doi.org/10.1016/j.nima.2012.03.015.

[21] W. Schweika, N. Violini, K. Lieutenant, C. Zendler, D. Nekrassov, A. Houben, P. Jacobs, P.F. Henry, DREAM-a versatile powder diffractometer at the ESS, J. Phys. Conf. Ser. 746 (2016). https://doi.org/10.1088/1742-6596/746/1/012013.

[22] K.H. Kleno, K. Lieutenant, K.H. Andersen, K. Lefmann, Systematic performance study of common neutron guide geometries, Nucl. Instruments Methods Phys. Res. Sect. A Accel. Spectrometers, Detect. Assoc. Equip. 696 (2012) 75–84. https://doi.org/10.1016/j.nima.2012.08.027.

[23] L.D. Cussen, D. Nekrassov, C. Zendler, K. Lieutenant, Multiple reflections in elliptic neutron guide tubes, Nucl. Instruments Methods Phys. Res. Sect. A Accel. Spectrometers, Detect. Assoc. Equip. 705 (2013) 121–131. https://doi.org/10.1016/j.nima.2012.11.183.

[24] J. Voigt, E. Babcock, T. Brückel, Beam transport and polarization at TOPAS, the thermal time-of-flight spectrometer with polarization analysis, J. Phys. Conf. Ser. 211 (2010) 6–12. https://doi.org/10.1088/1742-6596/211/1/012032.

[25] M. Bertelsen, The automatic neutron guide optimizer guide_bot, Nucl. Instruments Methods Phys. Res. Sect. A Accel. Spectrometers, Detect. Assoc. Equip. 867 (2017) 195–203. https://doi.org/10.1016/j.nima.2017.06.012.

[26] C. Zendler, K. Lieutenant, D. Nekrassov, M. Fromme, VITESS 3-virtual instrumentation tool for the European spallation source, J. Phys. Conf. Ser. 528 (2014). https://doi.org/10.1088/1742-6596/528/1/012036.

[27] P. Böni, High intensity neutron beams for small samples, J. Phys. Conf. Ser. 502 (2014). https://doi.org/10.1088/1742-6596/502/1/012047.

[28] K. Lieutenant, L.D. Cussen, Beam transport in double elliptic neutron guides, J. Neutron Res. 18 (2015) 127–134. https://doi.org/10.3233/JNR-160033.

[29] S. Mattauch, A. Koutsioubas, U. Rücker, D. Korolkov, V. Fracassi, J. Daemen, R. Schmitz, K. Bussmann, F. Suxdorf, M. Wagener, P. Kämmerling, H. Kleines, L. Fleischhauer-Fuß, M. Bednareck, V. Ossoviy, A. Nebel, P. Stronciwilk, S. Staringer, M. Gödel, A. Richter, H. Kusche, T. Kohnke, A. Ioffe, E. Babcock, Z. Salhi, T. Bruckel, The high-intensity reflectometer of the jülich centre for neutron science: MARIA, J. Appl. Crystallogr. 51 (2018) 546–654. https://doi.org/10.1107/S1600576718006994.

[30] M. Bertelsen, H. Jacobsen, U. Bengaard Hansen, H. Hoffmann Carlsen, K. Lefmann, Exploring performance of neutron guide systems using pinhole beam extraction, Nucl. Instruments Methods Phys. Res. Sect. A Accel. Spectrometers, Detect.

Assoc. Equip. 729 (2013) 387–398. https://doi.org/10.1016/j.nima.2013.07.062.